Journal of Saudi Chemical Society (2022) **26**, 101422

King Saud University

Journal of Saudi Chemical Society

www.ksu.edu.sa
www.sciencedirect.com

ORIGINAL ARTICLE

Lime peel extract induced $NiFe_2O_4$ NPs: Synthesis to applications and oxidative stress mechanism for anticancer, antibiotic activity

Abdul Raouf Malik [a], Muhammad Hammad Aziz [b], Muhammad Atif [c], Muhammad Sultan Irshad [d], Hafeez Ullah [a,e], Tuan Nguyen Gia [f], Hijaz Ahmed [g,h], Shafiq Ahmad [i], Thongchai Botmart [j,*]

[a] *Institute of Physics, The Islamia University of Bahawalpur, Bahawalpur 63100, Pakistan*
[b] *Department of Physics, COMSATS University Islamabad, Lahore Campus, Lahore 54000, Pakistan*
[c] *Department of Physics and Astronomy, College of Science, King Saud University, P O Box 2455, Riyadh 11451, Saudi Arabia*
[d] *Ministry-of-Education Key Laboratory for the Green Preparation and Application of Functional Materials, Hubei Key Laboratory of Polymer Materials, School of Materials Science and Engineering, Hubei University, Wuhan 430062, PR China*
[e] *Institute of Physics, Biophotonics Imaging Techniques Laboratory, The Islamia University of Bahawalpur, Bahawalpur 63100, Pakistan*
[f] *Department of Computing, University of Turku, 20500 Turku, Finland*
[g] *Information Technology Application and Research Center, Istanbul Ticaret University, 34445 Istanbul, Turkey*
[h] *Department of Mathematics, Faculty of Humanities and Social Sciences, Istanbul Ticaret University, 34445 Istanbul, Turkey*
[i] *Industrial Engineering Department, College of Engineering, King Saud University, P.O. Box 800, Riyadh 11421, Saudi Arabia*
[j] *Department of Mathematics, Faculty of Science, Khon Kaen University, Khon Kaen 40002, Thailand*

Received 12 October 2021; revised 3 January 2022; accepted 6 January 2022
Available online 17 January 2022

KEYWORDS

Nickel ferrites;
Green synthesis;
Anticancer;
Antimicrobial;
Cytotoxicity;
Reactive Oxygen Species (ROS) phenomenon

Abstract Nanobiotechnology, joined with green science, has incredible potential for the advancement of novel and important products that benefit human health, climate, and industries. Green chemistry of materials from synthesis to diverse biomedical applications is a talk of town in today's sustainable ideal world. Green synthesized nickel ferrites nanoparticles via biogenic lime peel extract (LPE) are investigated with precision and complete trail has been reported as multiple efficacies. The fcc crystal structure with the crystallite size (31 nm) were accessed by the XRD, magnetic properties using VSM, and FTIR for the functional group analysis of $NiFe_2O_4$ nanoparticles mediated by Lime peel extract ($NiFe_2O_4$@LPE NPs). From TEM and SEM analysis the average

* Corresponding author at: Department of Mathematics, Faculty of Science, Khon Kaen University, Khon Kaen 40002, Thailand.
E-mail addresses: hammadaziz@cuilahore.edu.pk (M.H. Aziz), hafeezullah@iub.edu.pk (H. Ullah), thongbo@kku.ac.th (T. Botmart).

Peer review under responsibility of King Saud University.

Production and hosting by Elsevier

https://doi.org/10.1016/j.jscs.2022.101422

diameter of the NPs was observed in the range of 31–35 nm. In 3D view, the surface morphology was analyzed by the AFM. $NiFe_2O_4$@LPE NPs were used to assess cytotoxicity and cellular morphological alterations in *In Vitro* cervical cancerous cells (HeLa). Nanosized $NiFe_2O_4$@LPE accompanied the considerable NPs topology induced dose dependent MMP in HeLa cells unlike the previous interpretation of controlled metabolism anticancer activity for HeLa cancerous cells. Therefore, it is referred by oxidative stress and reduction phenomena for anticancer effects and inactivation of carcinogen. Moreover, Antioxidant DPPH radical scavenging method and antibacterial *Bacillus subtilis*, *Escherichia coli*, *Pseudomonas aeruginosa*, and *Staphylococcus aureus* activity were observed in the synthesized nickel ferrites NPs.

1. Introduction

Nanotechnology is an emerging yet novel field of exploration in which particles that range in size from about 1–100 nm are synthesized and assigned. To add, Nanotechnology is an advance form of research area amalgamating different fields like chemistry, photography, biology, medicine, and engineering in it [1–3]. As explained, Nano biotechnology is vast and an evolving area where this multidisciplinary field allows the best use of many biomedical applications such as green methodologies to make benefit out of the nanoparticles [4–11]. In the recent past, there has been an enormous amount of work done in this area of biosynthesis of metal nanostructures that served a range of services, to put some as instance, bio imaging, anticancer effects, water treatment or catalysis [12–14]. Among all the range of the nanostructures that are biosynthesized, the nanoparticles of nickel, copper, iron, cobalt, and manganese are remarkable and distinguishing as these are highly promising substances are full of unique and enriched properties [15].

Nanoparticles with magnetic properties evolved the whole diversity of research work because they are highly applicable in various scientific advances including the biomedical field as well. It is used in medicine at various steps such as drug delivery, chemotherapy, phototherapy, and magnetic resonance imaging as well as applying targeted therapeutics [16,17]. When external magnetic field is provided to such cases, such systems of NPs can be easily and more efficiently controlled. The sensitivity of NPs can be enhanced which is directly proportional to the surface to volume ratio of NPs and hence can increase the colloidal stability and targeting of magnetic ferrites nanostructure [18]. Among all the available ferrites, Nickel ferrite (NiFe2O4) is the only ferrite with an inverted spinel structure and is also known as a solid magnetic material due to its high saturation magnetism and magneto crystalline anisotropy. Due to its remarkably great anisotropy with physical and chemical stability, it has been the most commonly and widely used ferrite in biomedical applications [19,20].

Lime peel is important as its ethnopharmacology is diverse including the antifungal, antibacterial, antioxidant, anticancer and enormous radical scavenging affects. Lime peel when in the form of extract contains flavonoids, Gallic acid and terpenoids all of which are known catalysts for speeding up redox reactions. For the synthesis of $NiFe2O_4$ nanostructures, there have been many studies making use of chemical synthesis techniques like as sol–gel, microwave, electrospinning, co-precipitation, and combustion methods [21–23]. All the above mentioned chemical methods are not devoid of having shortcomings, to name a few, such as requirement of expensive equipment's, significant energy consumption and depending on chemical compounds which are known as notorious to the environment and living beings on the Earth [24]. It is hence, the need of the time, to explore and discover newer as well as simpler techniques that are comparably, compatible to environment, cheaper, non-toxic and more attainable for the synthesis of such types of nanoparticles. Green synthesis methods have several advantages over chemical synthesis methods, including ease of access, a quick one-step process, lower external energy consumption, low cost, quick synthesis process, non-toxicity, and environmental friendly [22–25]. Another point to ponder that the solvents or agents that are used in biomolecule-assisted process are nontoxic. These in turn saves the environment from causing any damage to the atmosphere [22–26]. Hence, the major purpose of this study is to use lime peel extract in the synthesis of bio- and ecological $NiFe_2O_4$ NPs and the method used is green synthesis. Moreover, biocompatible functionalities that are part of the lime peel extract served as functional reducing and coating agent. Also, this work observed the cytotoxicity of $NiFe_2O_4$@LPE nanoparticles by noticing the reactive oxygen species and mitochondrial membrane potential activities. Moreover, such $NiFe_2O_4$@LPE nanoparticles has come out causing the effective antibacterial response against different pathogens.

2. Experimental

2.1. Materials

Nickel nitrate $Ni(NO_3)_2{\cdot}6H_2O$ (99.99%), ferric nitrate Fe $(NO_3)_2{\cdot}9H_2O$ (99.95%), ethanol (C_2H_5OH), 2,2-diphenyl-1-picrylhydrazyl (DPPH), acetic acid (CH_3COOH) and sodium hydroxide (NaOH) were purchased from Sigma Aldrich. Deionized and distilled water were also used in the experiment.

2.2. Lime peel extract preparation

The 50 g of the lime peel was first washed with running tap water, then distilled water. The peel was chopped into the small pieces and boiled in 300 ml distilled water for 30 min on hotplate. The solution was filtered through filter paper and the pale-yellow aqueous lime peel extract (LPE) was stored in the freezer. This LPE was further used in the green synthesis of the ferrites as the fuel instead of the chemicals.

2.3. Green synthesis of nickel ferrites

The nickel ferrites ($NiFe_2O_4$) NPs were green synthesized using the sol–gel auto combustion route. In green synthesis, lime peel extract was used as the ecofriendly fuel instead of chemicals. The precursor salts, 3 g of $Ni(NO_3)_2{\cdot}6H_2O$ and 20 g of $Fe(NO_3)_2{\cdot}9H_2O$ were separately dissolved in the 100 ml of distilled water under stirring. The prepared solutions mixed and then kept further stirring for 1 h. For ecofriendly approach, 30 ml of the lime peel extract was added and initially maintain the pH > 9 of the solution by using the 0.5 M solution of NaOH. After that the mixture was positioned on hot plate at 100 °C and stirred continuously until the thick gel formed. The obtained gel was further heated up to 150 °C temperature in oven and the gel was dried and converted into the powdered form. The obtained powder grinded, sintered at 700 °C for 2 h to eliminate the impurities and finally obtained the NiFe2O4@LPE nanoparticles.

2.4. Antioxidant activity

Antioxidant activity of $NiFe_2O_4$ @ LPE NPs was investigated by 2,2-diphenyl-1-picrylhydrazyl (DPPH) radical scavenging assay as reported in previous studies [26,27]. The different concentrations (10 μg/ml, 20 μg/ml, 40 μg/ml, 60 μg/ml, 80 μg/ml and 100 μg/ml) of $NiFe_2O_4$ @ LPE NPs were used for antioxidant study. 2 ml of each sample was added into the 1.5 ml of the DPPH 100 μM in ethanol. Then, the absorbance of the nanoparticles and DPPH mixture solution was noted down at 517 nm by utilizing the UV–visible spectrometer.

The following relationship was used to calculate the antioxidant activity.

$$DPPHradicalscaveningactivity(\%) = \frac{Abs(DPPH) - Abs(S)}{A(DPPH)}$$

Here, Abs (DPPH) and Abs(S) is the absorbance of the DPPH solution and samples $NiFe_2O_4$ @ LPE NPs mixture with DPPH solution respectively.

2.5. Anticancer activity

2.5.1. Cell culturing and exposure with $NiFe_2O_4$ @ LPE NPs

During in the cell culture procedure, HeLa cells were cultured in T75 flasks. Minimum Essential Medium (MEM) was mixed with 2 ml glutamine, 10 ml fetal bovine serum after which 10% Hanks salts were added [27]. Furthermore, the cells were cultured for 24 h at 37 °C to ensure the proper substratum connection. Cells were incubated to subculturing once or twice a week. When these cells reached 75–85 percent confluence, trypsin was used to collect them. The HeLa cells were cultured for 24 h on 96 well plates before being treated. $NiFe_2O_4$ @ LPE Nanoparticles were dissolved and then placed in cell culture medium to reach at desired ratio.

2.5.2. Measurement of in vitro cellular cytotoxicity, MTT assay

The human cervical cancer HeLa cells were implanted on a 96-well culture plate and cultured inside the incubator at 37 °C in the presence of 5% carbon dioxide CO2. They were incubated for 24 h after being treated (with or without) with varying quantities of NiFe2O4 @ LPE nanoparticles ranging from 10 to 125 μg/mL. Each well was exposed to the MTT assay, and then 30 μL of MTT (20 mg/ml) were added and incubated it for 5 h. The cells were distributed in 100 μL solvent of dimethyl sulphoxide after the medium was removed. By using microplate reader absorbance spectra of the synthesized material was analyzed at the wavelength of 595 nm. Measurements of cell viability were reported as a percentage of control values as reported in previous studies [28–33].

2.5.3. Morphological cellular analysis

HeLa cells were plated in six-well plates with 1 × 104 cells per well and then treated for 12 h to green produced NiFe2O4 @ LPE NPs at varied concentrations to perceive the malignant cells shape. Inverted phase contrast microscopy at 20× magnification was used to examine morphological changes caused by NiFe2O4 @ LPE NPs in HeLa cells [28].

2.5.4. $NiFe_2O_4$@LPE in HeLa cells staining of Prussian blue

HeLa cells were first planted in a 35 mm plate and then incubated for 24 h in different doses of $NiFe_2O_4$@LPE (25 μg/ml, 50 μg/ml, and 100 μg/ml). The cells were dyed with Prussian blue as described in previous studies to observe the intracellular of NiFe2O4@LPE nanoparticles with a light microscope. The cells were washed three times in PBS before being fixed for 30 min in 4% paraformaldehyde. After fixation with PBS and 15 min of staining with Perl's Prussian blue 2% potassium ferrocyanide ($C_6FeK_4N_6$) in 6% aqueous hydrochloric acid (HCl), the same washing procedure was repeated. The stained cells were rinsed again in PBS before being counterstained with nuclear fast red for 5 min. Finally, a light microscope was used to examine the stained HeLa cells that had been treated with NiFe2O4@LPE [34,35].

2.5.5. Mitochondrial membrane potential (MMP)

Mitochondrial membrane potential was evaluated by using the procedure reported [36]. Briefly, HeLa cells 5 × 10^4 cells/well were incubated for 12 h with different quantities of $NiFe_2O_4$@LPE (0, 25, 50 and 100 μg/ml). Rh-123 dye was utilized to evaluate mitochondrial variation by using a fluorescence microscope at 40× magnification for the morphological changes [27].

2.6. Antibacterial activity by disk-diffusion method

Antibacterial activity of the $NiFe_2O_4$ @ LPE nanoparticles were tested by following the disk-diffusion method. In disk-diffusion method Muller-Hinton agar was used as the medium by preparing the agar petri plate. 38 g of the agar powder was diluted in 100 ml of distilled water and autoclaved at 121 °C for 15 min. Afterward, it was well mixed and put into the petri plates and placed at room temperature for cooling. For antibacterial study of $NiFe_2O_4$ @ LPE NPs, the different concentrations 20 μg/ml, 50 μg/ml and 80 μg/ml were prepared and cotton disk soaked in the saline solutions to prepare the sample disk. The bacterial strains gram positive (i.e., *S. aureus*, *B. subtilis*) and gram negative (i.e., *E. coli*, *K. pneumonia*) were tested. Then, the strains were spread over the agar plates with the help of cotton swab. The prepared $NiFe_2O_4$ @ LPE NPs filter disk of different concentrations were pasted on the agar plate gently and incubate them at 37 °C for 24 h. The bacteri-

cidal potential of the $NiFe_2O_4$ @ LPE NPs have been found by measuring the zone of inhibition.

2.7. Material characterizations

The phase formation and particle size of NiFe2O4 were investigated using an X-ray diffractometer CuK_α radiations, PANalytical X'Pert-PRO (Tokyo, Japan). Transmission electron microscopy (TEM) (JEOL 2010, USA), operating voltage 100 kV and scanning electron microscope (SEM), Hitachi S-4800 were used to examine the morphology of $NiFe_2O_4$ @ LPE NPs. Atomic force microscopy (AFM) image was also obtained by silicon cantilevers in contact mode. Magnetic characteristics were investigated by Vibrating sample magnetometer (VSM). The possible functional groups of $NiFe_2O_4$ @ LPE NPs were identified using Fourier-transform infrared (FTIR) in the 400–4000 cm^{-1} range. The crystallite size of green prepared $NiFe_2O_4$ NPs was estimated using Scherer's formula.

$$D = K\lambda/\beta os\theta$$

2.8. Statistical analysis

The observed data were calculated as the mean standard deviation for three different observations. The observed facts were evaluated using the student's *t*-test. The calculated p-value was less than 0.05 was done via Excel software and determined as statistically significant.

3. Results and discussion

3.1. Characterization's analysis of $NiFe_2O_4$ @ LPE NPs

The XRD analysis of green produced $NiFe_2O_4$ @ LPE nanoparticles indicated the crystalline face -centered cubic (fcc) phase spinel structure. The mentioned structure is followed with accurate JCPDS NO-54-0964. The observed peaks are situated with 2θ values at 30.2°, 35.8°, 37.4°, 43.3°, 53.7°, 57.3°, and 63.4° with associated plain indices (220), (311), (222), (400), (422), (511) and (440) which is shown in Fig. 1(a). The average crystallite size of prepared NPs was determined using Scherer's formula which came out to be 31 nm. The structure of the green synthesized $NiFe_2O_4$ @ LPE nanoparticles shows the nanosized particle dimension.

FTIR spectroscopy was done in nickel ferrites as shown in Fig. 1(b) from 4000 to 400 cm^{-1} range for the existence of chemical bonding. At 3348 cm^{-1} the stretching band confirms the presence of O–H bonds that confirms the main contribution in the synthesis. The stretching at 2918 cm^{-1} and 2850 cm^{-1} are due to the presence of hydrogen bonding as a component of lime peel extract [27]. Small aberrations in the range 2362–2200 cm^{-1} reveals the N–H bonds which confirms the presence of amine salts present in lime peel extract. On the other hand, stretching of 1578 cm^{-1} confirms the presence of C–C bonds and aberrations at 1414 cm^{-1} shows the C-H_3 groups [35–40]. The stretching range within 650–430 cm^{-1} indicates the existence of nickel ferrites. The band at 650 cm^{-1} shows the tetrahedral structure of nickel ferrites mediated by lime peel extract in this stretching range [36].

TEM was used to investigate the internal nanostructured analysis of NiFe2O4, as shown in Fig. 2(a). Synthesized $NiFe_2O_4$ nanoparticles are continually sized, uniform, and randomly distributed with grain size of 33–35 nm. A slight difference of about 31–35 nm almost confirmed the size calculated from XRD patterns using Debye Scherer's formula. The obtained SEM images of $NiFe_2O_4$@LPE NPs indicate the layered porous structure of the synthesized nano-sized ferrites as shown in Fig. 2(b). As a result, both SEM and TEM analysis indicated that the prepared $NiFe_2O_4$@LPE having nanostructures which supports each other.

The atomic force microscopy (AFM) technique using to examine the surface texture of $NiFe_2O_4$ @ LPE nanoparticles, which is significant for determining the roughness of the surface of $NiFe_2O_4$@LPE nanoparticles for reducing ability and formulation as a capping agent. The morphology and surface texture of $NiFe_2O_4$ @ LPE nanoparticles as shown 2D & 3D view in Fig. 2(c-d). Statistical analysis of surface morphology was performed using Gwydion software which revealed the average waviness (47 pm) and average surface roughness (4.1 pm) because of green synthesis and it is negligible as compared to the high roughness of simple $NiFe_2O_4$ NPs [36–39]. As a result, the surface image of $NiFe_2O_4$ NPs confirmed their spherical shape which is further verified by SEM and TEM images. The observed morphology of green synthesized nickel ferrites could be useful in a variety of applications including bio-medical devices, water purification, and antibacterial agents [40–42].

The magnetic characteristics of the $NiFe_2O_4$ @ LPE nanoparticles is revealed by thin S-shaped M-H loops. Magnetically soft ferrites have many applications in EMI suppression, radar cross section and micro-wave absorption. The intrinsic magnetic properties of the given M-H loops i.e. saturation magnetization, magnetic remanence and magnetic coercivity were measured as shown in the Fig. 3.

The intrinsic magnetic characteristics of $NiFe_2O_4$ @ LPE NPs are influenced by the magnetic anisotropy field, grain size, porosity, and sintering temperature. Such low magnetization and magnetic remanence levels have been discovered [36,41]. Measured coercivity of the green synthesized nickel ferrite is 207.01 Oe. The number of pores has a direct relationship with magnetic properties like remanence and coercivity. Coercivity increases as the number of pores increase [42,43]. On the other hand, the Hc values less than 500 O_e are considered extremely helpful for high-frequency microwave applications. The anisotropy constant (K) can be determined by using the measured values of M_s and H_c by the formulas.

$$K = \frac{\mathrm{MsxHc}}{0.96} \quad (1)$$

3.2. Antioxidant activity of $NiFe_2O_4$ @ LPE NPs

The DPPH radical scavenging assay technique was used to assess the antioxidant activity of $NiFe_2O_4$@LPE NPs. Fig. 4 shows that $NiFe_2O_4$ nanoparticles have high antioxidant activity at various concentrations, but that the findings are inferior to ascorbic acid at larger doses. According to another research, it is revealed that copper ferrite ($CuFe_2O_4$) and zinc ferrite ($ZnFe_2O_4$) demonstrated resilience-free radical scavenging properties in comparison to ascorbic acid [36]. At the concen-

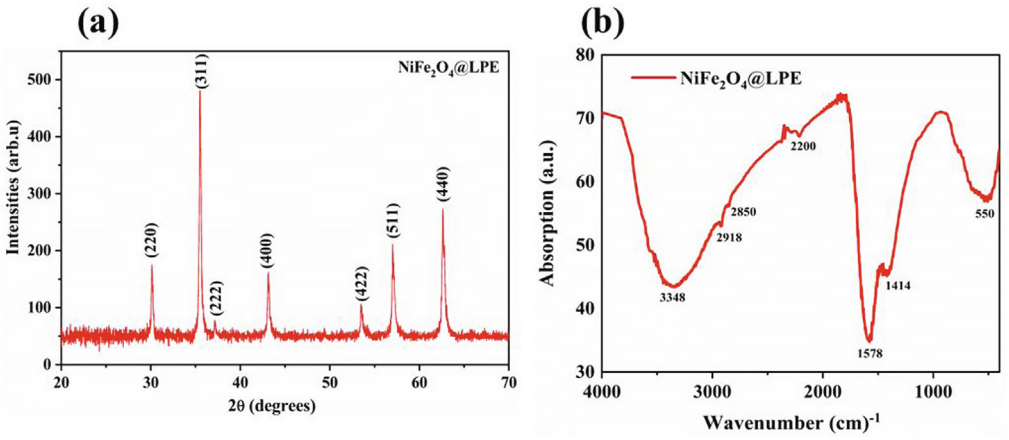

Fig. 1 (a) XRD pattern of green synthesized $NiFe_2O_4$ @ LPE NPs. (b) FTIR spectrum of $NiFe_2O_4$@LPE NPs which shows the presence of primary constituents of nickel ferrites.

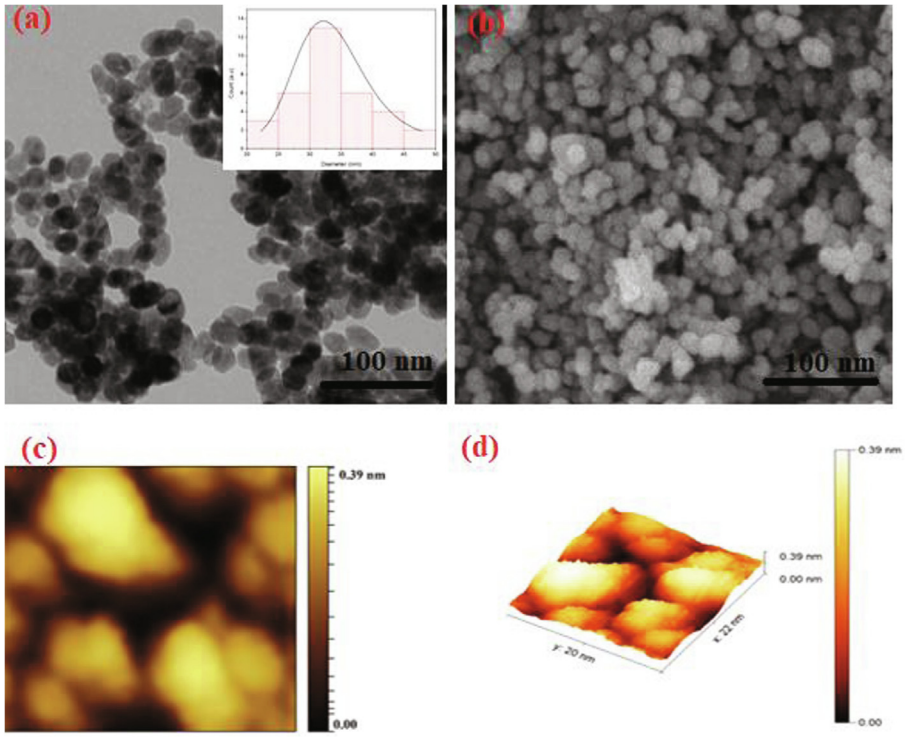

Fig. 2 Morphological profile of green synthesized $NiFe_2O_4$ @ LPE NPs (a) TEM image revealing internal structural morphology (b) SEM showing surface morphology (c) 2D AFM image reveals the surface topography and (d) 3D view of $NiFe_2O_4$ @ LPE NPs.

tration of 125 µg/ml ascorbic acid (58.13% ± 1.54%) was assessed as a potent scavenging agent along with nanoparticles of $ZnFe_2O_4$ (30.58%) and $CuFe_2O_4$ (28.67% ± 1.15%). The concentration of nanoparticles was increased, which resulted in an increase in antioxidant activity. Antioxidant activity is always expressed as the movement of free electrons from the oxygen atom of nanoparticles to free radicals located at the nitrogen atom of DPPH molecules [44,45].

In our study, the presence of phenolic and flavonoid chemicals in lime peel extract (LPE), which eventually releases free-radicals and is thus ascribed as DPPH scavengers, is one of the most intriguing candidates for radical scavenging activity [46–49]. Previous studies have proved that various metallic nanoparticles have been found to exhibit antioxidant characteristics for scavenging free radicals. A high surface to volume ratio is also suggested to be one of the promising explanations for antioxidant activity in certain nanoparticles [46–48]. These findings could be supported by the relatively strong antioxidant behavior of Co Fe_2O_4, Fe_3O_4, and NiO nanoparticles in contrast to their bulk state [46,47,50,51]. The findings of this

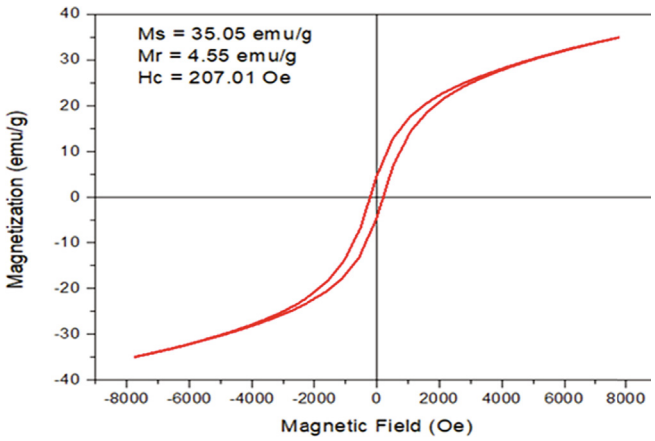

Fig. 3 M vs H loops for synthesized $NiFe_2O_4$@LPE NPs with maximum H-field to be 8 KOe.

study are positive in this regard, and they provide a starting point for further research into NiFe2O4 as a potential antioxidant candidate.

3.3. Anticancer activity

The cytotoxicity of $NiFe_2O_4$ against HeLa cells, as well as the possibility of spectacular cell death, were thoroughly examined. Gallic acid, ethyl gallate, ellagic acid, chebulinic acid, and luteolin are the cytotoxic phenolic chemicals found in lime peel extract [49]. Previous research has looked into the anticancer properties of phenolic compounds in HeLa cancer cells via regulating their metabolic processes. Oxidative reduction is a potential phenomenon that allows phenolic compounds to have anticancer effects, carcinogen inactivation, and metastasis inhibition [45,47–49]. Therefore, the most effective technique for testing cytotoxicity against HeLa cancerous cells is to use nickel ferrite nanoparticles in combination with lime peel extract. Implementation of $NiFe_2O_4$@LPE to HeLa cells resulted in loss of cell viability and proliferation. The MTT assay was used to determine cellular viability at different dosages of $NiFe_2O_4$@LPE NPs for 24 h. In Fig. 5 (a), cell viability is reduced in the order of 91%, 77%, 68%, 59%, 46 and 38% when HeLa cells were exposed to $NiFe_2O_4$ @ LPE NPs at 20, 40, 60, 80,100 and 120 μg/ml concentrations, respectively.

Also, indicated similar results were demonstrated by earlier published studies, in which biosynthesized nanoparticles were shown to have cytotoxicity potential [33,34,44]. Fig. 6 depicts the morphological mutants of HeLA cells exposed for 24 h to green synthesized $NiFe_2O_4$@LPE NPs at varying concentrations.

As compared to control HeLa cells, the effect of $NiFe_2O_4$@LPE was detected as morphological changes at higher concentrations. HeLa cells shrank and lost their usual shape after being exposed to $NiFe_2O_4$@LPE NPs, as well as a loss in cell adhesion capacity and density. Using plant-derived metal oxide or magnetic ferrites NPs, previous research indicated cellular morphological damage in a variety of cancerous cell lines [33,34,44].

Fig. 7 shows Prussian blue-stained HeLa cells cultured in the presence of green produced $NiFe_2O_4$. Fig. 7(a–d) shows a photomicrograph of Prussian blue-stained HeLa cells showing the buildup of $NiFe_2O_4$NPs on the cell surface. These $NiFe_2O_4$@LPE demonstrate the progressive increase of accretion for the doses of 25 μg/ml, 50 μg/ml and 100 μg/ml after an incubation time of 12 h. Interestingly, these accumulation

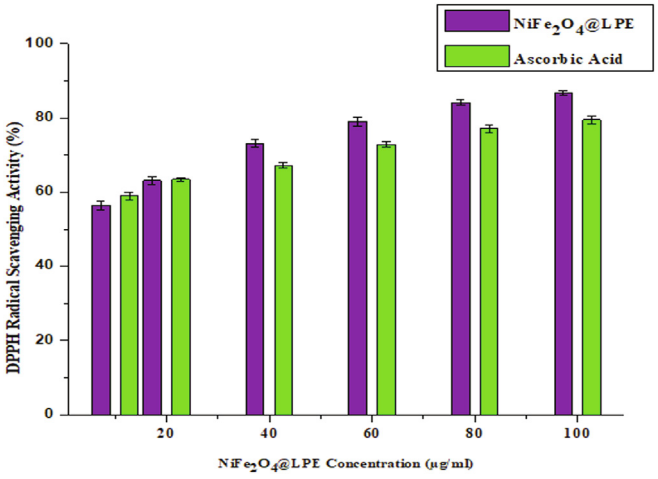

Fig. 4 DPPH radical scavenging activity of ascorbic acid and $NiFe_2O_4$ nanoparticles mediated by lime peel extract.

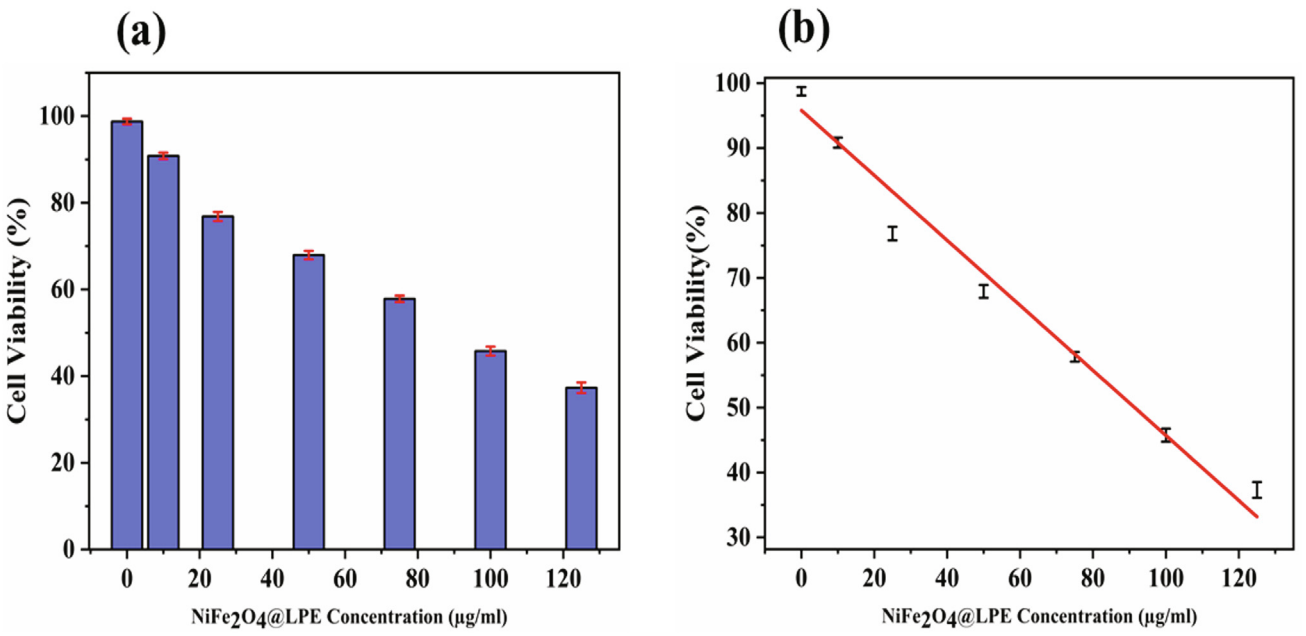

Fig. 5 (a) Represent the cellular viability (%) of HeLa cells when treated with $NiFe_2O_4$@LPE NPs after 24 h, *t*-test (*p < 0.05) (b) demonstrate the linear calibration plot of $NiFe_2O_4$@LPE NPs vs cell viability.

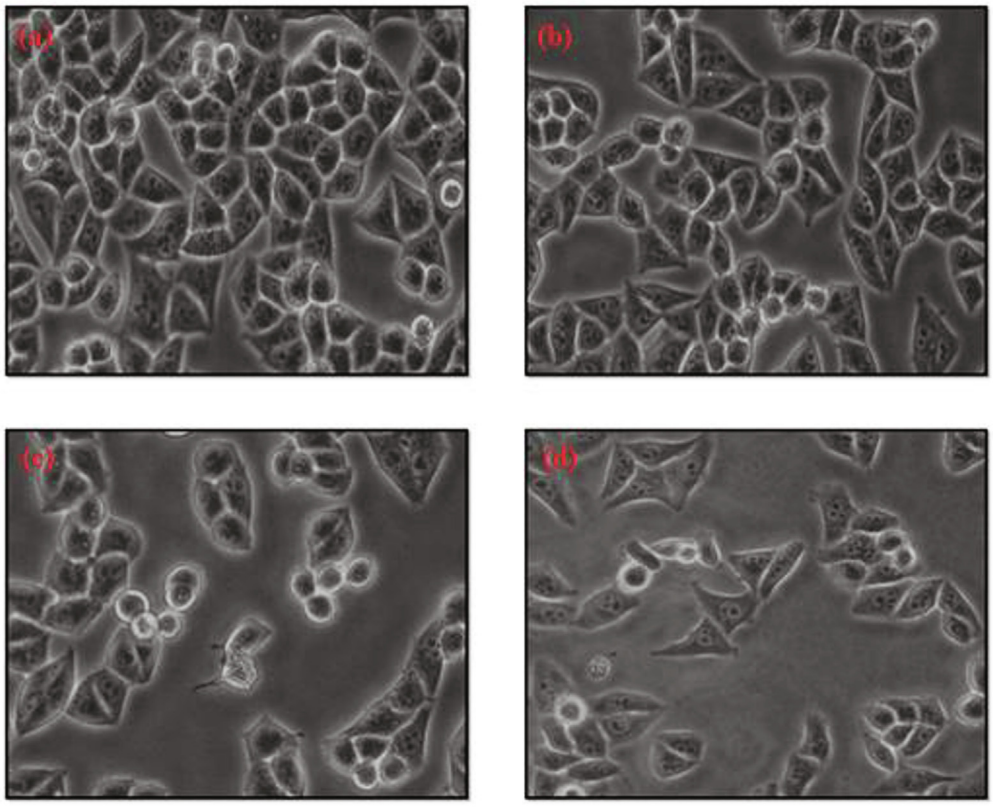

Fig. 6 The morphological variations of HeLa cells which caused by green synthesized $NiFe_2O_4$@LPE NPs at various doses (a) control (b) 25 µg/ml (c) 50 µg/ml (d) 100 µg/ml.

results show that $NiFe_2O_4$@LPE NPs were efficiently accumulated in the cytoplasm of marked HeLa cells.

Numerous research has looked at the impact of reactive oxygen species in causing cellular loss by damaging the mitochondrial membrane [50–59]. It's important to note that the mitochondrial membrane potential of cancerous cells reduces during apoptosis. As shown in Fig. 8, MMP level was used as a biomarker for apoptosis in HeLa cancerous

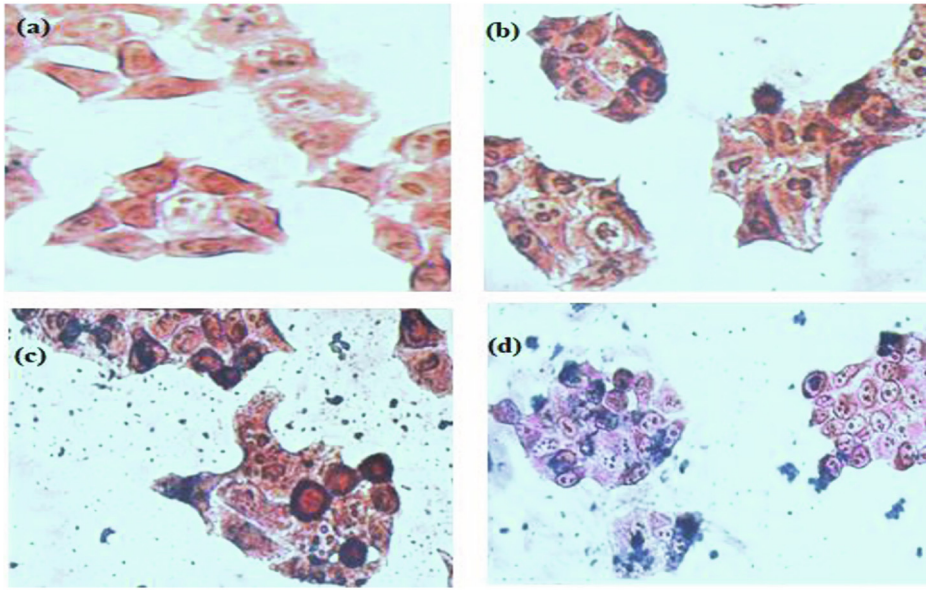

Fig. 7 Photomicrographs of HeLa cells after 12 h by Prussian blue staining of when exposed with NiFe2O4@LPE NPs (a) control (b) 25 μg/ml (c) 50 μg/ml (d) 100 μg/ml.

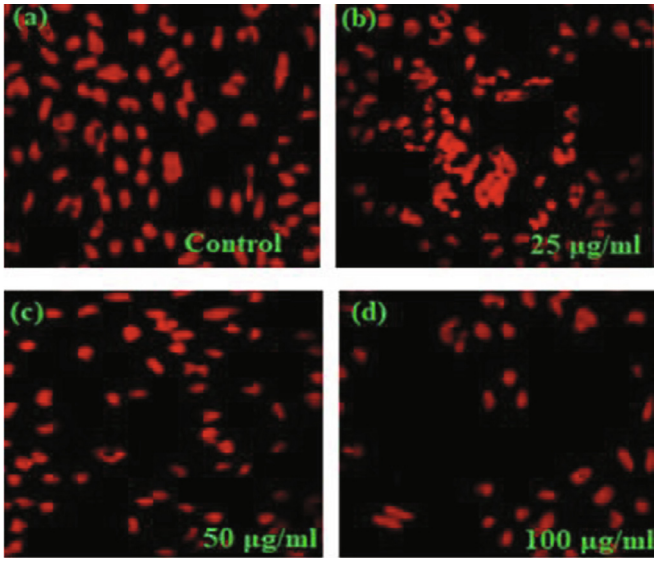

Fig. 8 Illustrative morphological variations displaying $NiFe_2O_4$@LPE NPs induced MMP in HeLa cells in dose-dependent way a) control (b) 25 μg/ml (c) 50 μg/ml (d) 100 μg/ml.

cells after 12 h of exposure to $NiFe_2O_4$@LPE at different doses ranging from 25 to 100 μg/ml. Using the Rh123 dye, a significant morphological difference in MMP level in Hela cells is detected. These morphological impacts revealed a dose-dependent increase of MMP levels in $NiFe_2O_4$@LPE compared to control, indicating a function for ROS production as well as oxidative stress against HeLa cells [37,38,45].

3.4. Antibacterial activity of $NiFe_2O_4$@LPE NPs

By using the disk-diffusion technique, $NiFe_2O_4$@LPE nanoparticles were exposed with 20 μg/ml, 50 μg/ml, and 80 μg/ml correspondingly. The results of in vitro examinations of $NiFe_2O_4$LPE revealed that as concentrations increased, the antibacterial reaction increased. Conventional antibacterial materials like antibiotic tetracycline ($C_{22}H_{24}N_2O_8$) and dimethyl sulphur oxide (C_2H_6OS) were used as a control. The antibiotic concentrations were maintained constant at 0.005 mg/mL, while the concentrations of NiFe2O4@LPE NPs were 20 μg/ml, 50 μg/ml, and 80 μg/ml, accordingly. Furthermore, lime peel extract contains flavonoids and therefore by increasing the concentrations of $NiFe_2O_4$@LPE NPs improves antibacterial activity enhances the zone of inhibition against gram-positive and gram-negative bacteria, as shown in Fig. 9(a).

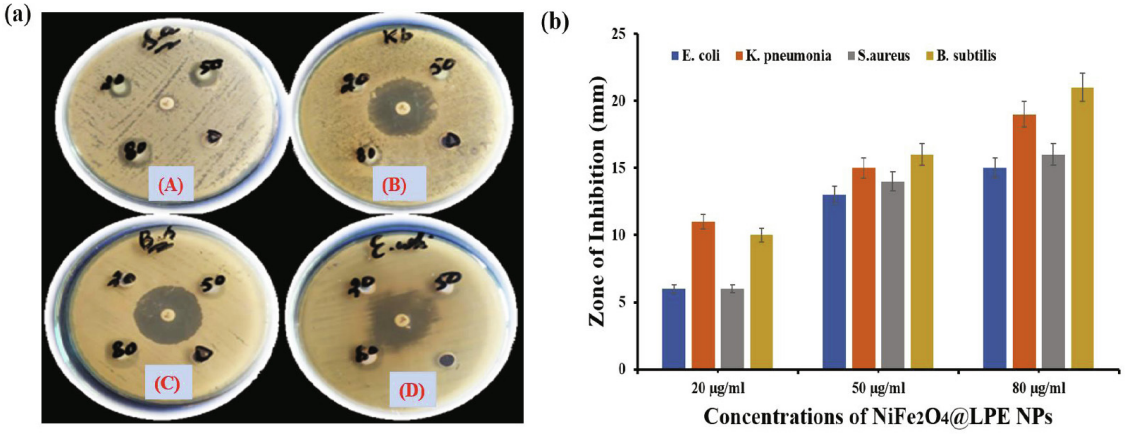

Fig. 9 (a) Antibacterial activity of $NiFe_2O_4$@LPE NPs against different microbial strains at different concentrations with accordance to positive and negative control. A). S. aureus B) klebsiella pneumonia C) bacillus subtilis D) E. coli. (b) Histogram represents the comparison for zone of inhibition for increasing concentrations of nanoparticles.

In comparison to other bacteria such as *E. coli* and *S. aureus*, the zone of inhibition against *B. subtilis* and *K. pneumonia* appears to be greater. Fig. 9(b) shows the superior antibacterial activity against *B. subtilis* and *K. pneumonia* when each value was tested three times and taken in triplicates with standard deviation. These findings indicate that $NiFe_2O_4$ can connect to the cell wall, causing cell rupture by altering membrane permeability [38,60,61]. Manju et al. also discovered the antibacterial activity of mixed copper-nickel ferrites mediated by lime juice, which revealed a powerful antibacterial agent against a variety of pathogenic microorganisms [62].

4. Conclusion

The study has marked the protocol for facile green synthesis of $NiFe_2O_4$ nanoparticles mediated through a biogenic reducing agent of lime peel extract for the first time. The synthesized $NiFe_2O_4$@LPE NPs have shown anticancer potential against human cervical cancer (HeLa) cells as revealed in the concentration-dependent cytotoxicity, ROS, and MMP in HeLa cells. The morphology in AFM and Nanosized vesicle in TEM results escorted the considerable NPs topology induced dose-dependent MMP in HeLa cells. Contrary to previous reports where anticancer activity against HeLa cancerous cells discussed referring the controlled metabolic activities. Our study revealed the underlying oxidative stress and reduction phenomena for anticancer effects and inactivation of carcinogen. The report further established that synthesized $NiFe_2O_4$ NPs possess effective antibacterial activity against Gram-positive and Gram-negative bacteria. Hence, our findings highlighted from synthesis to application that lime peel extract can be used as reducing and stabilizing agent for Nanoscale synthesis of $NiFe_2O_4$ which further offer noticeable potential as antioxidant, anticancer, and antibacterial activities. Nevertheless, rapid communication of the present study can draw the focus and attention of contemporary researchers to number of important biological applications in cancer therapy, drug delivery, and magnetic resonance imaging (MRI) for unprecedented results in coming years.

Acknowledgement

Researchers Supporting Project number (RSP-2021/397), King Saud University, Riyadh, Saudi Arabia.

Conflicts of interest

None.

References

[1] K. McNamara, S.A.M. Tofail, Nanosystems: the use of nanoalloys, metallic, bimetallic, and magnetic nanoparticles in biomedical applications, Phys. Chem. Chem. Phys. 17 (2015) 27981–27995.
[2] N.T.K. Thanh, N. Maclean, S. Mahiddine, Mechanisms of nucleation and growth of nanoparticles in solution, Chem. Rev. 114 (15) (2014) 7610–7630.
[3] M. Holzinger, A. Le Goff, S. Cosnier, Nanomaterials for biosensing applications: a review, Front. Chem. 2 (2014) 63.
[4] R. Watkins, L. Wu, C. Zhang, R.M. Davis, B. Xu, Natural product-based nanomedicine: recent advances and issues, Int. J. Nanomed. 10 (2015) 6055.
[5] A.G. Ingale, A.N. Chaudhari, Biogenic synthesis of nanoparticles and potential applications: an eco-friendly approach, J. Nanomed. Nanotechol. 4 (2013) 1–7.
[6] M. Khan, M. Kuniyil, M.R. Shaik, M. Khan, S.F. Adil, A. Al-Warthan, H.Z. Alkhathlan, W. Tremel, M.N. Tahir, M.R.H. Siddiqui, Plant extract mediated eco-friendly synthesis of pd@graphene nanocatalyst: An efficient and reusable catalyst for the Suzuki-Miyaura coupling, Catalysts 7 (2017) 1–14, https://doi.org/10.3390/catal7010020.
[7] M. Shaik, G. Albalawi, S. Khan, M. Khan, S. Adil, M. Kuniyil, A. Al-Warthan, M. Siddiqui, H. Alkhathlan, M. Khan, "Miswak" based green synthesis of silver nanoparticles: Evaluation and comparison of their microbicidal activities with the chemical synthesis, Molecules 21 (11) (2016) 1478, https://doi.org/10.3390/molecules21111478.
[8] M. Khan, M.R. Shaik, S.T. Khan, S.F. Adil, M. Kuniyil, M. Khan, A.A. Al-Warthan, M.R.H. Siddiqui, M. Nawaz Tahir, Enhanced antimicrobial activity of biofunctionalized zirconia nanoparticles, ACS Omega 5 (4) (2020) 1987–1996, https://doi.org/10.1021/acsomega.9b03840.

[9] A.A. Mostafa, S.R.M. Sayed, E.N. Solkamy, M. Khan, M.R. Shaik, A. Al-Warthan, S.F. Adil, Evaluation of biological activities of chemically synthesized silver nanoparticles, J. Nanomater. 2015 (2015) 1–7, https://doi.org/10.1155/2015/789178.

[10] M. Asimuddin, M.R. Shaik, S.F. Adil, M.R.H. Siddiqui, A. Alwarthan, K. Jamil, M. Khan, Azadirachta indica based biosynthesis of silver nanoparticles and evaluation of their antibacterial and cytotoxic effects, J. King Saud Univ. - Sci. 32 (1) (2020) 648–656, https://doi.org/10.1016/j.jksus.2018.09.014.

[11] S. Saif, A. Tahir, T. Asim, Y. Chen, M. Khan, S.F. Adil, Green synthesis of ZnO hierarchical microstructures by Cordia myxa and their antibacterial activity, Saudi, J. Biol. Sci. 26 (7) (2019) 1364–1371, https://doi.org/10.1016/j.sjbs.2019.01.004.

[12] J.K. Patra, K.-H. Baek, Green nanobiotechnology: factors affecting synthesis and characterization techniques, J. Nanomater. 2014 (2014) 1–12.

[13] L.S. Arias, J.P. Pessan, A.P.M. Vieira, T.M.T. de Lima, A.C.B. Delbem, D.R. Monteiro, Iron oxide nanoparticles for biomedical applications: a perspective on synthesis, drugs, antimicrobial activity, and toxicity, Antibiotics 7 (2018) 46.

[14] K.D. Arunachalam, S.K. Annamalai, Chrysopogon zizanioides aqueous extract mediated synthesis, characterization of crystalline silver and gold nanoparticles for biomedical applications, Int. J. Nanomed. 8 (2013) 2375.

[15] J. Singh, T. Dutta, K.-H. Kim, M. Rawat, P. Samddar, P. Kumar, 'Green'synthesis of metals and their oxide nanoparticles: applications for environmental remediation, J. Nanobiotechnol. 16 (2018) 84.

[16] R.A. Revia, M. Zhang, Magnetite nanoparticles for cancer diagnosis, treatment, and treatment monitoring: recent advances, Mater. Today 19 (3) (2016) 157–168.

[17] A. Curcio, A.K.A. Silva, S. Cabana, A. Espinosa, B. Baptiste, N. Menguy, C. Wilhelm, A. Abou-Hassan, Iron oxide nanoflowers@ CuS hybrids for cancer tri-therapy: Interplay of photothermal therapy, magnetic hyperthermia and photodynamic therapy, Theranostics 9 (2019) 1288.

[18] K. Turcheniuk, A.V. Tarasevych, V.P. Kukhar, R. Boukherroub, S. Szunerits, Recent advances in surface chemistry strategies for the fabrication of functional iron oxide based magnetic nanoparticles, Nanoscale 5 (22) (2013) 10729, https://doi.org/10.1039/c3nr04131j.

[19] J.-L. Ortiz-Quiñonez, U. Pal, M.S. Villanueva, Structural, magnetic, and catalytic evaluation of spinel Co, Ni, and Co–Ni ferrite nanoparticles fabricated by low-temperature solution combustion process, ACS Omega 3 (11) (2018) 14986–15001.

[20] C. Dey, A. Chaudhuri, A. Ghosh, M.M. Goswami, Magnetic cube-shaped NiFe2O4 nanoparticles: an effective model catalyst for nitro compound reduction, ChemCatChem. 9 (2017) 1953–1959.

[21] N. Narang, W. Jiraungkoorskul, Anticancer activity of key lime, Citrus aurantifolia, Pharmacogn. Rev. 10 (2016) 118.

[22] YuQiu Liu, E. Heying, S.A. Tanumihardjo, History, global distribution, and nutritional importance of citrus fruits, Compr. Rev. Food Sci. Food Saf. 11 (6) (2012) 530–545.

[23] C. Caristi, E. Bellocco, V. Panzera, G. Toscano, R. Vadalà, U. Leuzzi, Flavonoids detection by HPLC-DAD-MS-MS in lemon juices from Sicilian cultivars, J. Agric. Food Chem. 51 (12) (2003) 3528–3534.

[24] D. Hong, Y. Yamada, M. Sheehan, S. Shikano, C.-H. Kuo, M. Tian, C.-K. Tsung, S. Fukuzumi, Mesoporous nickel ferrites with spinel structure prepared by an aerosol spray pyrolysis method for photocatalytic hydrogen evolution, ACS Sustain. Chem. Eng. 2 (11) (2014) 2588–2594.

[25] O.V. Kharissova, H.V.R. Dias, B.I. Kharisov, B.O. Pérez, V.M. J. Pérez, The greener synthesis of nanoparticles, Trends Biotechnol. 31 (4) (2013) 240–248.

[26] A. Ebrahiminezhad, A. Zare-Hoseinabadi, A.K. Sarmah, S. Taghizadeh, Y. Ghasemi, A. Berenjian, Plant-mediated synthesis and applications of iron nanoparticles, Mol. Biotechnol. 60 (2) (2018) 154–168.

[27] E. Fröhlich, Comparison of conventional and advanced in vitro models in the toxicity testing of nanoparticles, Artif. Cells, Nanomed. Biotechnol. 46 (2018) 1091–1107.

[28] F. Ibraheem, M.H. Aziz, M. Fatima, F. Shaheen, S.M. Ali, Q. Huang, In vitro Cytotoxicity, MMP and ROS activity of green synthesized nickel oxide nanoparticles using extract of Terminalia chebula against MCF-7 cells, Mater. Lett. 234 (2019) 129–133.

[29] M. Atif, W.A. Farooq, M.A. Siddiqui, A.A. Al-Khedhairy, Preliminary study of spectral features of normal and malignant cell cultures, Laser Phys. 26 (4) (2016) 045601, https://doi.org/10.1088/1054-660X/26/4/045601.

[30] M. Atif, A.R. Malik, M. Fakhar-e-Alam, S.S. Hayat, S.S.Z. Zaidi, R. Suleman, M. Ikram, In vitro studies of Photofrin®mediated photodynamic therapy on human rhabdomyosarcoma cell line (RD), Laser Phys. 22 (1) (2012) 286–293, https://doi.org/10.1134/S1054660X11230010.

[31] M. Atif, M. Fakhar-e-Alam, S. Firdous, S.S.Z. Zaidi, R. Suleman, M. Ikram, Study of the efficacy of 5-ALA mediated photodynamic therapy on human rhabdomyosarcoma cell line (RD), Laser Phys. Lett. 7 (10) (2010) 757–764, https://doi.org/10.1002/lapl.201010061.

[32] M. Atif, M. Fakhar-e-Alam, S.S.Z. Zaidi, R. Suleman, Study of the efficacy of photofrin®-Mediated PDT on human hepatocellular carcinoma (HepG2) cell line, Laser Phys. 21 (6) (2011) 1135–1144.

[33] M. Atif, A.R. Malik, M. Fakhar-e-Alam, S.S. Hayat, S.S.Z. Zaidi, R. Suleman, M. Ikram, In vitro studies of Photofrin® mediated photodynamic therapy on human rhabdomyosarcoma cell line (RD), Laser Phys. 22 (1) (2012) 286–293.

[34] R. Wang, J. Liu, Y. Liu, R. Zhong, X. Yu, Q. Liu, L. Zhang, C. Lv, K. Mao, P. Tang, The cell uptake properties and hyperthermia performance of Zn0. 5Fe2. 5O4/SiO2 nanoparticles as magnetic hyperthermia agents, R. Soc. Open Sci. 7 (2020) 191139.

[35] J.A. Heredia-Guerrero, J.J. Ben\'\itez, E. Dom\'\inguez, I.S. Bayer, R. Cingolani, A. Athanassiou, A. Heredia, Infrared and Raman spectroscopic features of plant cuticles: a review, Front. Plant Sci. 5 (2014) 305.

[36] S. Laurent, D. Forge, M. Port, A. Roch, C. Robic, L. Vander Elst, R.N. Muller, Magnetic iron oxide nanoparticles: synthesis, stabilization, vectorization, physicochemical characterizations, and biological applications, Chem. Rev. 108 (2008) 2064–2110.

[37] G. Karunakaran, M. Jagathambal, N. Van Minh, E. Kolesnikov, D. Kuznetsov, Green synthesis of NiFe2O4 spinel-structured nanoparticles using Hydrangea paniculata flower extract with excellent magnetic property, JOM 70 (7) (2018) 1337–1343.

[38] R. Zandipak, S. Sobhanardakani, Synthesis of NiFe2O4 nanoparticles for removal of anionic dyes from aqueous solution, Desalin. Water Treat. 57 (24) (2016) 11348–11360.

[39] T.M. Naidu, P.V.L. Narayana, Synthesis and characterization of Fe-TiO2 and NiFe2O4 nanoparticles and its thermal properties, J. Nanosci. Technol. 5 (4) (2019) 769–772.

[40] S. Sagadevan, Z.Z. Chowdhury, R.F. Rafique, Preparation and characterization of nickel ferrite nanoparticles via co-precipitation method, Mater. Res. 21 (2) (2018), https://doi.org/10.1590/1980-5373-mr-2016-0533.

[41] A.A. Khan, M. Javed, A.R. Khan, Y. Iqbal, A. Majeed, S.Z. Hussain, S.K. Durrani, Influence of preparation method on structural, optical and magnetic properties of nickel ferrite nanoparticles, Mater. Sci. 35 (2017) 58–65.

[42] P. Sivakumar, R. Ramesh, A. Ramanand, S. Ponnusamy, C. Muthamizhchelvan, Synthesis and characterization of nickel

ferrite magnetic nanoparticles, Mater. Res. Bull. 46 (12) (2011) 2208–2211.
[43] I. Zalite, G. Heidemane, J. Grabis, M. Maiorov, The synthesis and characterization of nickel and cobalt ferrite nanopowders obtained by different methods, Powder Technol. 97 (2018).
[44] S. Kanagesan, M. Hashim, S.A.B. Aziz, I. Ismail, S. Tamilselvan, N.B. Alitheen, M.K. Swamy, B. Purna Chandra Rao, Evaluation of antioxidant and cytotoxicity activities of copper ferrite (CuFe2O4) and zinc ferrite (ZnFe2O4) nanoparticles synthesized by sol-gel self-combustion method, Appl. Sci. 6 (2016) 184.
[45] I. Khalil, W.A. Yehye, A.E. Etxeberria, A.A. Alhadi, S.M. Dezfooli, N.B.M. Julkapli, W.J. Basirun, A. Seyfoddin, Nanoantioxidants: Recent trends in antioxidant delivery applications, Antioxidants 9 (2020) 24.
[46] S. Paul, J.P. Saikia, S.K. Samdarshi, B.K. Konwar, Investigation of antioxidant property of iron oxide particlesby 1′-1′ diphenylpicryl-hydrazyle (DPPH) method, J. Magn. Magn. Mater. 321 (21) (2009) 3621–3623.
[47] D. Das, B.C. Nath, P. Phukon, A. kalita, S.K. Dolui, Synthesis of ZnO nanoparticles and evaluation of antioxidant and cytotoxic activity, Colloids Surfaces B Biointerfaces 111 (2013) 556–560.
[48] L. Valgimigli, A. Baschieri, R. Amorati, Antioxidant activity of nanomaterials, J. Mater. Chem. B 6 (14) (2018) 2036–2051.
[49] D.A. Zema, P.S. Calabrò, A. Folino, V. Tamburino, G. Zappia, S.M. Zimbone, Valorisation of citrus processing waste: A review, Waste Manag. 80 (2018) 252–273.
[50] J.P. Saikia, S. Paul, B.K. Konwar, S.K. Samdarshi, Nickel oxide nanoparticles: a novel antioxidant, Colloids Surf. B Biointerfaces 78 (1) (2010) 146–148.
[51] Y. Liu, L. Yu, Y. Hu, C. Guo, F. Zhang, X. Wen Lou, A magnetically separable photocatalyst based on nest-like γ-Fe 2O 3/ZnO double-shelled hollow structures with enhanced photocatalytic activity, Nanoscale 4 (2012) 183–187, https://doi.org/10.1039/c1nr11114k.
[52] D.B. Zorov, M. Juhaszova, S.J. Sollott, Mitochondrial reactive oxygen species (ROS) and ROS-induced ROS release, Physiol. Rev. 94 (3) (2014) 909–950.
[53] M. Xia, Y. Zhang, K. Jin, Z. Lu, Z. Zeng, W. Xiong, Communication between mitochondria and other organelles: a brand-new perspective on mitochondria in cancer, Cell Biosci. 9 (2019) 1–19.
[54] M. Sriramulu, D. Shukla, S. Sumathi, Aegle marmelos leaves extract mediated synthesis of zinc ferrite: Antibacterial activity and drug delivery, Mater. Res. Express. 5 (2018) 115404.
[55] M. Atif, S. Iqbal, M. Fakhar-E-Alam, M. Ismail, Q. Mansoor, L. Mughal, M.H. Aziz, A. Hanif, W.A. Farooq, Manganese-doped cerium oxide nanocomposite induced photodynamic therapy in MCF-7 cancer cells and antibacterial activity, Biomed Res. Int. 2019 (2019) 1–13, https://doi.org/10.1155/2019/7156828.
[56] M. Atif, M. Fakhar-e-Alam, N. Abbas, M.A. Siddiqui, A.A. Ansari, A.A. Al-Khedhairy, Z.M. Wang, in vitro cytotoxicity of mesoporous SiO2 @Eu(OH)3 core-shell nanospheres in MCF-7, J. Nanomater. 2016 (2016) 1–6.
[57] M. Atif, S. Iqbal, M. Fakhar-e-Alam, Q. Mansoor, K.S. Alimgeer, A. Fatehmulla, A. Hanif, N. Yaqub, W.A. Farooq, S. Ahmad, H. Ahmad, Y. ming Chu, Manganese-doped cerium oxide nanocomposite as a therapeutic agent for MCF-7 adenocarcinoma cell line, Saudi, J. Biol. Sci. 28 (2021) 1233–1238, https://doi.org/10.1016/j.sjbs.2020.12.006.
[58] M. Fakhar-e-Alam, Aqrab-ul-Ahmad, M. Atif, K.S. Alimgeer, M. Suleman Rana, N. Yaqub, W. Aslam Farooq, H. Ahmad, Synergistic effect of TEMPO-coated TiO2 nanorods for PDT applications in MCF-7 cell line model, Saudi, J. Biol. Sci. 27 (12) (2020) 3199–3207, https://doi.org/10.1016/j.sjbs.2020.09.027.
[59] S. Iqbal, M. Fakhar-e-Alam, K.S. Alimgeer, M. Atif, A. Hanif, N. Yaqub, W.A. Farooq, S. Ahmad, Y.-M. Chu, M. Suleman Rana, A. Fatehmulla, H. Ahmad, Mathematical modeling and experimental analysis of the efficacy of photodynamic therapy in conjunction with photo thermal therapy and PEG-coated Au-doped TiO2 nanostructures to target MCF-7 cancerous cells, Saudi, J. Biol. Sci. 28 (2) (2021) 1226–1232, https://doi.org/10.1016/j.sjbs.2020.11.086.
[60] S. Maensiri, C. Masingboon, B. Boonchom, S. Seraphin, A simple route to synthesize nickel ferrite (NiFe2O4) nanoparticles using egg white, Scr. Mater. 56 (9) (2007) 797–800.
[61] N. Durán, A.B. Seabra, Metallic oxide nanoparticles: state of the art in biogenic syntheses and their mechanisms, Appl. Microbiol. Biotechnol. 95 (2012) 275–288.
[62] B.G. Manju, P. Raji, Green synthesis, characterization, and antibacterial activity of lime-juice-mediated copper–nickel mixed ferrite nanoparticles, Appl. Phys. A 126 (2020) 156.